Interfacial Layer Development in Hot-Dip Galvanneal Coatings on Interstitial Free (IF) Steel

C.E. JORDAN, K.M. GOGGINS, and A.R. MARDER

During the annealing of hot-dip galvanized coatings on interstitial free (IF) steel, an interfacial layer was found to develop and grow at the steel/coating interface. The interfacial layer followed a three-step growth process in which there was initial rapid growth up to a thickness of approximately 1.0 μm, followed by a period of essentially no growth with continued zinc and iron interdiffusion into the coating, and finally renewed growth at long time (60 second) anneals. The interfacial layer did not inhibit zinc and iron interdiffusion or the development of the Fe-Zn alloy layer. Coating iron content increased rapidly before the interfacial layer grew to a thickness of 1.0 μm, however, once the coating reached a total iron content in excess of 11.0 wt pct, interfacial layer growth became active and coating iron content increased only slightly with continued annealing. Although powdering of the coating as evaluated by a 60 deg bend test was generally found to increase with an increase in interfacial layer thickness, particularly in excess of 1.0 μm, no definitive relationship between interfacial layer thickness and powdering was found. The thickness of this interfacial layer, however, can be used as an indicator of formability performance.

I. INTRODUCTION

THE demand for zinc-coated steel sheet has risen dynamically in recent years due to an increase in the use of zinc-based coatings for corrosion resistant applications in the automotive industry. Zinc coatings provide cosmetic, perforation, and general atmospheric corrosion protection against such aggressive environmental conditions as road deicing salt and acid rain.[1] One type of zinc coating, an Fe-Zn alloyed coating, has had expanded use in the automotive industry because of its superior weldability, paintability, and cosmetic corrosion resistance over that of pure zinc coatings. Fe-Zn alloyed coatings are typically produced by annealing the coating after hot-dip galvanizing, electrogalvanizing, or zinc vapor deposition processes.

Hot-dip galvanneal is a hot-dip galvanized zinc coating that has been annealed to transform the almost pure zinc eta phase overlay to a fully alloyed Fe-Zn coating containing approximately 10 wt pct iron. The alloyed coating consists of various Fe-Zn intermetallic phases, including zeta, delta, gamma$_1$, and gamma$_2$. The phases that are present in a galvanneal coating are shown in the zinc-rich portion of the Fe-Zn equilibrium phase diagram (Figure 1).[2]

Although the introduction of iron into the zinc coating (especially at the surface of the coating) has been shown to result in beneficial paintability and weldability properties, the ductility of the coating deteriorates with increasing amounts of iron. The alloyed coating can fracture during deformation processes such as stamping and deep drawing, resulting in the exfoliation of the coating. The removal of the coating during forming operations is often referred to as powdering, and the formability of the coating is evaluated based on its resistance to powdering. During press-forming operations, the coating can powder or flake causing defects in the surface of the final coated product. In the case of hot-dip galvannealed coatings, the coating exfoliates and adheres to the press-forming dies, resulting in further damage to subsequently pressed parts and to the dies themselves.[1] A characteristic of galvanneal coatings which has been related to coating formability performance is the total iron content of the coating. Many researchers[3–7] have found that as the coating iron content increases, a corresponding increase is noted in the amount of powdering that occurs after bend testing of the coated sheet samples.

Recent studies have focused on the factors that affect intermetallic phase formation, with an emphasis upon optimizing coating formability. Simulation of the post hot-dip heat-treatment cycle of the galvanneal process has proven effective in understanding the structure development that occurs after galvanizing and during annealing.[7] Of particular interest to this structure development is the growth of an interfacial layer of Fe-Zn intermetallic gamma$_1$, and/or gamma$_2$ phase adjacent to the steel substrate. Gamma$_1$ and gamma$_2$ are the most iron-rich of the intermetallic phases that develop within the coating during the galvannealing process. In addition, gamma$_1$, gamma$_2$, and delta are the hardest and most brittle of the Fe-Zn phases that develop during annealing.[8] It is therefore believed by some researchers[9,10,11] that the interfacial location and thickness of the gamma phases adversely affect coating adhesion properties. The work presented here characterizes interfacial layer development and its role in determining the

C.E. JORDAN, Ph.D. Candidate, Department of Materials Science and Engineering, and A.R. MARDER, Professor, Department of Materials Science and Engineering, and Associate Director, Energy Research Center, are with Lehigh University, Bethlehem, PA 18015. K.M. GOGGINS, formerly Graduate Student, Department of Materials Science and Engineering, Lehigh University, is with the International Paper Company, Memphis, TN 38119.

Manuscript submitted August 23, 1993.

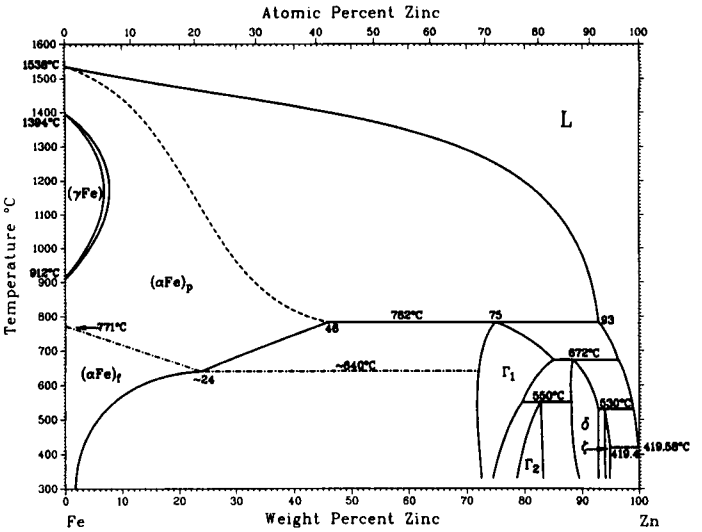

Fig. 1—Fe-Zn equilibrium phase diagram.[2]

formability properties of process-simulated galvanneal coatings.

II. EXPERIMENTAL PROCEDURE

A. *Process Simulation—Hot-Dip Galvanizing*

The chemical composition of the titanium stabilized interstitial free (IF) steel used in this study is shown in Table I. The sheet was coated on a hot-dip galvanizing pilot line at the Armco Research Center in Middletown, OH. The sheet speed through the pilot line was 6.4 m/min. In the first stage of the continuous pilot line, the cold-rolled sheet was recrystallization annealed between 650 °C and 760 °C in a gaseous 75 pct N_2 −25 pct H_2 reducing atmosphere, which had a dew point of −23 °C. The sheet was then hot-dip galvanized with an immersion time of approximately 8 to 9 seconds at a bath temperature of 460 °C. The galvanized coating weight averaged between 52 and 55 g/m^2 on each side of the sheet.

The galvanizing bath had an aluminum content of 0.10 effective weight percent.[12] Effective weight percent aluminum is the total aluminum content corrected for the oversaturation of iron in the zinc bath. The bath used in this study contained 0.03 wt pct Fe and had a total aluminum content of 0.11 wt pct. However, the solubility of iron in liquid Zn (0.11 wt pct Al) at 460 °C is 0.02 wt pct.[13] The effective Al in the bath was calculated using the bath chemical analysis data and a solubility equation developed by Guttman *et al.*[13] Effective Al content is a more accurate gage of the soluble aluminum that remains in the bath during galvanizing than is total aluminum content.[13]

B. *Process Simulation—Galvannealing*

In order to evaluate the coating structure development that occurs upon annealing, hot-dip galvanized steel sheet (0.08-cm thick × 5-cm wide × 22 cm-long) was treated under a variety of annealing temperature and hold time conditions using electric resistance heating in a Gleeble HAZ 1000. The samples were heated to the designated hold temperature at a rate of 500 °C/s in order to avoid any transformation before reaching the set annealing temperature. Three different annealing temperatures were studied, 450 °C, 500 °C, and 550 °C, with hold times varying between 1 and 60 seconds. After annealing, the samples were cooled to 300 °C at a rate of 25 °C/s using a water-mist quench to simulate a commercial in-line cooling cycle. A sample thermal profile is shown in Figure 2. The line designated as temperature program in Figure 2 represents the heat-treatment schedule that was programmed into the Gleeble. Temperatures 1 through 3 are readings taken from three thermocouples that were attached to the sheet specimen within the center 5 cm width × 6.5 cm lengthwise section to monitor the thermal profiles within that part of the sample. In addition to a thermocouple in the exact center of the sheet, two additional thermocouple (1.25 cm from each edge of the sample) were also positioned to monitor the edge-to-edge temperature gradient across the 5-cm wide section of the sample. These two thermocouples were 6.5 cm apart in the lengthwise direction of the sample and therefore could monitor temperature gradients in this direction as well. The center section followed the temperature program uniformly (±10 °C), and only this 5 × 6.5 cm region of the sample was used for metallographic, X-ray diffraction, and iron content analysis.

Table I. Substrate Chemical Analysis in Weight Percent (Balance Iron)

	C	Mn	S	P	N	Al	Si	Ti	Nb
Ti IF	0.004	0.13	0.005	0.003	0.003	0.049	0.004	0.078	<0.002

C. *Coating Characterization*

The metallographic preparation technique used a stack assembly of coated sheet samples in each mount to ensure that the entire cross section of the coating on all of the samples remained flat during grinding and polishing. Polishing was performed without using water as a lubricant or cleaning agent, and special care was taken to keep the samples extremely clean during preparation. A new etchant, which consists of a mixture of 1 pct picric acid in amyl alcohol and 1 pct nitric acid in amyl alcohol, was found to work well on all of the coatings studied. The metallographic technique used for sample preparation is described in detail elsewhere.[14]

Samples for X-ray analysis were sectioned from the Gleeble sheet specimen. Each sample was rotated within a PHILIPS* 3100 Diffractometer, and data were gathered from 2Θ angles between 25 and 85 deg at an angle increment of 0.01 deg and a scan rate of 1.0 deg/min. The source of radiation was copper K_α X-rays using generator settings of 45 kV and 30 mA. Only qualitative phase identification information was obtained from the X-ray diffraction analysis due to the severe overlap of the characteristic peaks associated with each Fe-Zn intermetallic phase.

*PHILIPS is a trademark of Philips Electronic Instruments Corp., Mahwah, NJ.

Another portion of the Gleeble sample was sectioned and subjected to a chemical titration method in order to determine the total iron content of the coating. A 10 pct sulfuric acid solution was used to dissolve the coating from the substrate steel. Complete coating removal was achieved when effervescing of the immersed sample was no longer observed. At this point, the sample was removed and the solution containing the dissolved coating was then titrated with a 0.01 N potassium permanganate solution. The volume of titrant used to equilibrate the solution and the weight difference of the sheet sample before and after coating removal were incorporated into the equation

$$\text{Weight percent iron} = \frac{[\text{volume of titrant (mL)} \cdot 5.585 \cdot 10^{-2}]}{[\text{coating weight (g)}]} \quad [1]$$

to determine the total weight percent iron present in the coating. The constant in Eq. [1] accounts for the concentration of the 10 pct sulfuric acid stripping solution and the 0.01 N potassium permanganate titrant used in the iron content determination.

Interfacial layer thickness measurements of the simulated galvanneal coatings were obtained using quantitative image analysis on the LECO* 2001 image analysis system. Samples which were prepared for light optical microscopy were examined using the light optical microscope attached to the LECO system, with no additional sample preparation. The LECO 2001 system digitizes the image from the light optical microscope and assigns gray levels (based on gray level contrast) to the image so that the feature of interest can be isolated based on its gray level and sized by a user-defined program.[15] The resolution limit of this image analysis technique was 0.4 μm for the measurement of interfacial layer thickness at 1500×. Three separate areas, each containing approximately 30 interfacial layer thickness measurements, were collected from each sample to establish mean and standard deviation values.

*LECO is a trademark of LECO Corporation, St. Joseph, MI.

D. *Powdering*

Powdering properties of the coating were evaluated after the simulated coatings were subjected to a 60 deg bend test (die tip diameter = 1.0 cm) on a 4206 Instron mechanical testing unit to a final load of 13,350 N. A schematic of the bend test apparatus is shown in Figure 3. To evaluate powdering, adhesive tape was placed on the surface of the sample directly opposite the contact surface of the male die prior to bending. Hence, the powdering data reported here were obtained from the side of the sheet that was in a compressive stress state during bending. After the bend test, the tape was removed and tested for light transmittance with a PERKIN-ELMER* Lambda 5 spectrophotometer. The degree of powdering for each specimen was evaluated by incorporating the

*PERKIN-ELMER is a trademark of Perkin-Elmer Physical Electronics, Eden Prairie, MN.

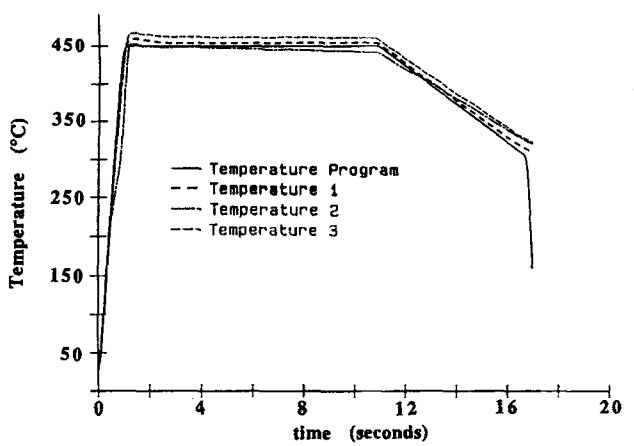

Fig. 2—An example thermal profile of an annealed sample processed on the Gleeble HAZ 1000.

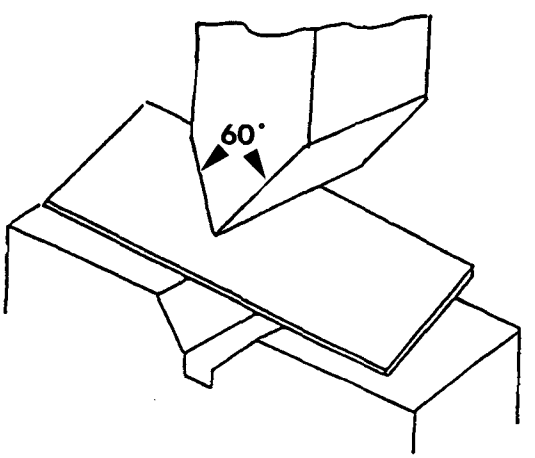

Fig. 3—Schematic drawing of the 60 deg bend test die configuration.

light transmittance measurement into a calculation for light absorbance (A), which can be defined as

$$A = \log (I_{100 \text{ pct transmittance}}/I_{\text{sample}}) \quad [2]$$

where $I_{100 \text{ pct transmittance}}$ is the intensity reading for light transmittance with no absorbance (light transmittance through a glass slide) and I_{sample} is the intensity of light transmitted through a glass slide containing the tape and exfoliated coating particles. Corrections for the transparency of the tape itself were accounted for in the measurement of light transmittance.[16] The powdering results are reported according to light absorbance and represent average values from five separate bend test samples.

III. RESULTS AND DISCUSSION

A. *Morphology Development*

Light optical microscopy of the annealed coatings in cross section revealed that the coatings exhibited transitions within the temperature-time testing matrix. The transition microstructures were classified in general to fit into three distinct morphological types: type 0, type 1, and type 2.[7,17] A schematic of each morphology type is shown in Figure 4. The following discussion on coating phase identification is based upon light optical microscopy examination, total coating iron content analysis, and X-ray diffraction data.

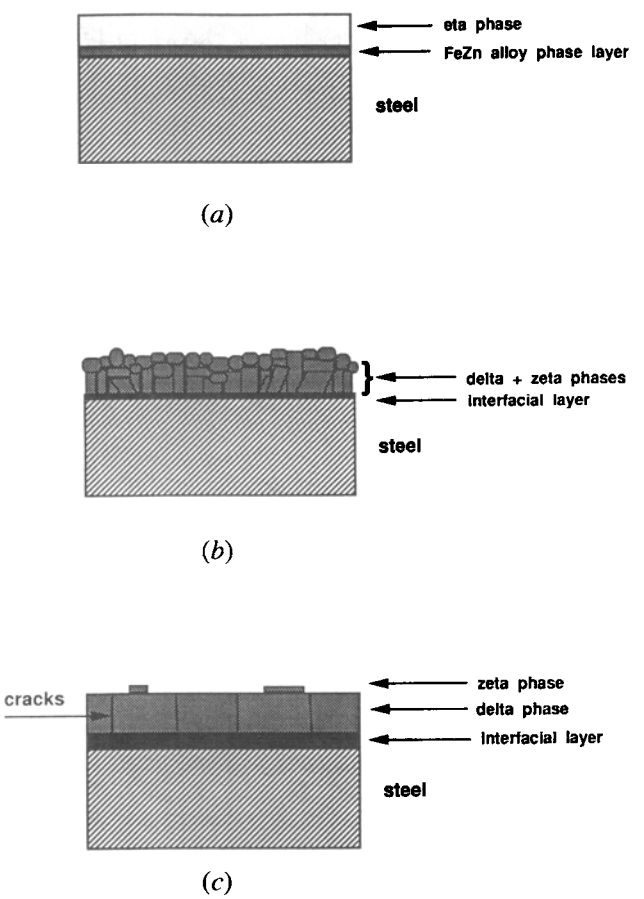

Fig. 4—Schematic representation of (*a*) type-0, (*b*) type-1, and (*c*) type-2 coating morphologies that form during annealing.

The type-0 microstructure is not a fully alloyed coating but has an overlay of pure eta phase that is approximately 8 to 9 μm in thickness, as shown in Figure 4(a). The type-0 structure also contains an Fe-Zn alloy layer (most likely delta and/or zeta phase) beneath the overlay that is approximately 1 to 2 μm in thickness. The Fe-Zn alloy layer grew at the expense of the eta phase overlay as the hold time of the anneal was increased. The type-1 microstructure, as shown in Figure 4(b), is a fully alloyed coating that develops at longer annealing times than the type-0 morphology and contains no apparent eta phase. The alloy layer in the type-1 morphology is most likely a mixed two-phase layer structure consisting of zeta and delta phase. An interfacial layer of less than 1.0 μm was also present in the type-1 coating morphologies on IF steel. The type-2 morphology (Figure 4(c)) is characterized by a thick compact delta phase layer and an interfacial layer most often greater than 1.0 μm thickness. The type-2 morphology frequently contained cracks perpendicular to the steel substrate. These cracks were inherent in the structure of the coating and not the result of sample preparation, as shown previously.[14]

In this study, the detailed morphological development was followed for the hot-dip galvanized (0.10 wt pct Al-Zn bath) Ti IF steel substrate. The coated steel was annealed at temperatures between 450 °C and 550 °C for 1 to 60 seconds in the Gleeble HAZ 1000, and the coating morphology development can be seen in Figures 5(a) through (o).

The morphological sequence in Figure 5 clearly reveals the development of the Fe-Zn alloy layer and an interfacial layer over the annealing cycles studied. The phase transformations that occur within the coating can be described through the use of the 450 °C annealed samples in Figures 5(a) through (e). During the initial stage of annealing, the galvanized coating forms an Fe-Zn alloy layer at the steel/coating interface (Figure 5(a)). From Figure 5(a) (type-0), it is apparent that the coating is not fully alloyed and that eta phase is present at the surface of the coating. Beneath the eta phase layer there exists a nonuniform layer consisting of delta phase with blocky crystals of zeta phase situated at the top part of this delta phase layer. The initially formed alloy layer grows over time (Figures 5(b) and (c)), consuming the eta phase overlay at the coating surface. The alloy layer at this stage is most likely a two-phase structure consisting of (1) delta phase near the steel/coating interface and (2) zeta phase at the surface of the coating. At this stage, an interfacial gamma layer of less than 1.0 μm has also developed at the steel/coating interface, as shown in Figure 5(c). The interfacial layer is most likely gamma_1 phase, but gamma_2 phase may also be present.[7,18] With continued annealing, the coating becomes fully alloyed and no eta phase remains at the surface of the coating, as shown in Figure 5(d) (type-1). The predominant phase in the coating at this stage of alloy layer development is a columnar-like layer that is delta phase.

Although the coating has undergone a morphology change from type-0 to type-1 during the 10-second interval between Figures 5(c) and (d), essentially no growth of the interfacial layer has occurred during this time. Prolonged annealing of this fully alloyed coating during the 40-second interval between Figure 5(d) (type-1) and

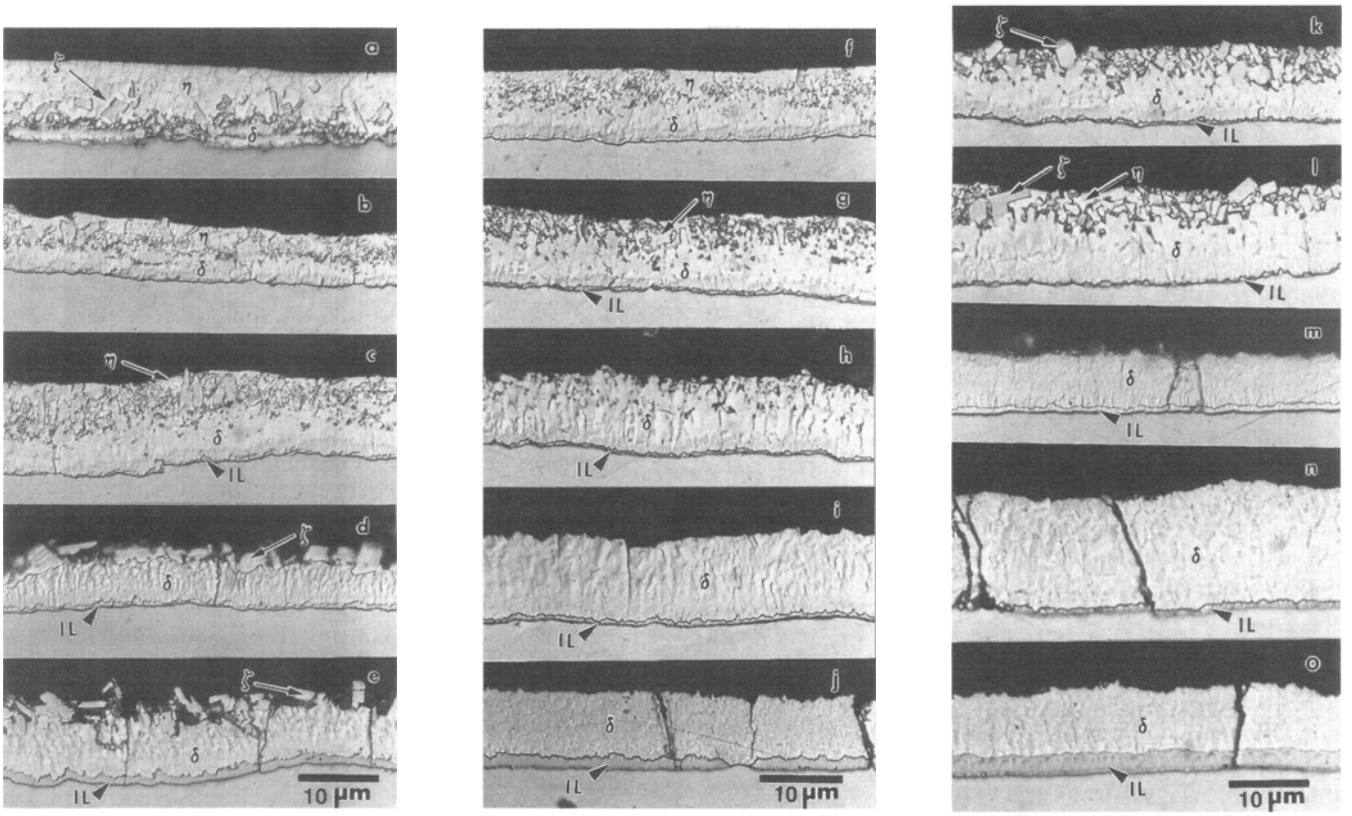

Fig. 5—Morphology development of the hot-dip galvanized Ti-stabilized IF steel annealed at (*a*) through (*e*) 450 °C for 1, 5, 10, 20, and 60 s, respectively; (*f*) through (*j*) 500 °C for 1, 5, 10, 20, and 60 s; and (*k*) through (*o*) 550 °C for 1, 5, 10, 20 and 60 s (IL = interfacial layer).

Figure 5(e) (type-2) results in the solid-state growth of the interfacial gamma layer. The significant growth of the interfacial layer at long time anneals was accompanied by the formation of cracks perpendicular to the steel/coating interface, which propagated through both the delta and $gamma_1/gamma_2$ layer. This sequence of alloy layer development was similar for the 500 °C and 550 °C annealed samples as well, as shown in Figures 5(f) through (j) (500 °C) and Figures 5(k) through (o) (550 °C).

In summary, the interfacial layer only exhibited significant solid-state growth after the delta phase had become the main constituent of the Fe-Zn alloy layer. Although the 500 °C and 550 °C annealed samples showed the formation of an interfacial layer after 5- and 1-second anneals, respectively, the interfacial layer did not show substantial growth until the coating became fully alloyed (no eta phase remained) and the delta layer became the major constituent of the Fe-Zn alloy layer.

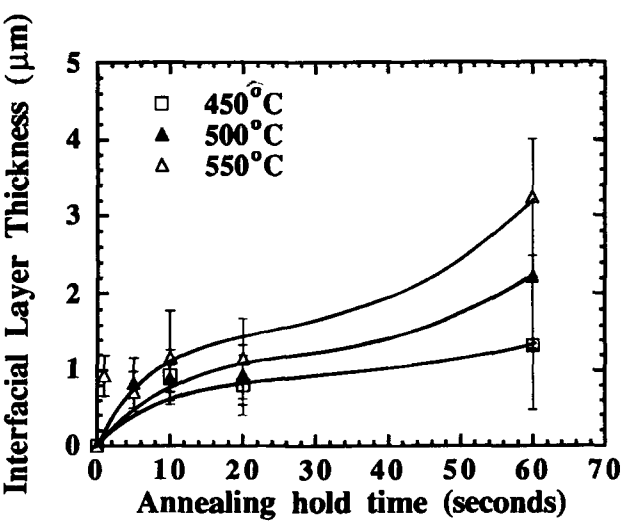

Fig. 6—Interfacial layer thickness data for the simulation galvannealed coatings.

B. *Growth of the Interfacial Layer*

The relationship between interfacial layer thickness and annealing hold time is shown in Figure 6. All three annealing temperatures exhibited the same relationship between interfacial layer thickness and annealing time. Initially, a rapid increase in interfacial layer growth was observed, followed by a steady-state region with almost no growth, and then by another increase in the growth rate after 20 seconds of annealing.

C. *Iron Content*

Total coating iron content as a function of annealing time is shown in Figure 7. Iron enrichment increases rapidly at short times of up to 20 seconds, after which the rate of zinc and iron interdiffusion begins to decrease. The change in the rate at which iron is introduced into the coating corresponds to an iron content of 10 to 13 wt pct.

D. *Relationship between Interfacial Layer Growth and Iron Content*

In comparing Figures 6 and 7, it is evident that during the 5- to 20-second anneals, the interfacial layer thickness remained essentially constant as the total iron content in the coating increased with time. When the coatings were annealed for greater than 20 seconds, however, the interfacial layer thickness increased with time, while the rate of increase in coating iron content was found to only slightly increase (Figures 6 and 7). Because both iron content and interfacial layer thickness appeared to exhibit a transition in behavior after a 20-second anneal, the relationship between these two coating variables was explored in detail.

Figure 8 correlates the change of interfacial layer thickness with coating iron content. Error bars for the interfacial layer thickness measurements in Figure 8 denote a one standard deviation value (1σ) both above and below the associated average interfacial layer thickness data point. The correlation of iron content data with interfacial layer thickness indicates that the iron content in the coating increased from 6 to 11 wt pct with no corresponding growth of the interfacial layer. According to the data shown in Figure 8, the interfacial layer does not influence zinc and iron interdiffusion into the coating. Once the coating iron content reached approximately 11 wt pct, however, significant growth of the interfacial layer commenced.

E. *Interfacial Layer Development*

Stage 1: *formation of the interfacial layer*

Initially, the as-galvanized coating consists entirely of eta phase, which serves as the source of zinc atoms for the growing Fe-Zn intermetallic phases during the early stages of galvannealing. The Fe-Zn phases initially nucleate at the steel/coating interface and consume the eta-phase layer as they grow. The interfacial gamma layer was found to nucleate and grow rapidly to an average thickness of approximately 1.0 μm during its first stage of development. Interfacial layer development was often observed before the coating was completely alloyed, for example, a 1-second anneal at 550 °C (Figure 5(k)).

Stage 2: *no growth of the layer—steady state*

After the initial formation and rapid growth stage, a steady-state period of continued zinc and iron interdiffusion with no growth of the interfacial layer occurred. The plateau regions of Figures 6 and 8 correspond to this second stage of interfacial layer development. During this arrested growth stage, the interfacial layer does not appear to inhibit zinc and iron interdiffusion or alloy layer development of the coating.

In this steady-state regime, eta and/or zeta phase at the coating surface are consumed by the growing delta layer. After the coating completely alloyed and all of the eta phase had been consumed, the predominant Fe-Zn intermetallic compound in the coating was found to be delta phase, based upon metallographic observation and X-ray diffraction data. The delta phase region of the equilibrium Fe-Zn phase diagram (Figure 1) has an iron solubility of up to about 12.0 wt pct. This solubility limit corresponds to approximately the same iron content at which the third and final step of interfacial layer growth occurred. As seen in Figure 8, this period of zinc and iron interdiffusion with no interfacial layer growth terminated when the coating iron content reached approximately 11.0 wt pct.

Stage 3: *solid-state growth of the layer*

During stage 2 development, iron that entered the coating led to a compact delta-phase morphology and additionally may have resulted in iron saturation of the delta phase. After a short time of no interfacial layer growth (plateau region in Figure 6), solid-state growth becomes active and the thickness of the interfacial layer increases (last region in Figure 6). The beginning of this third and final stage of interfacial layer development may be related to iron saturation of the delta-phase layer, as discussed subsequently.

At the end of stage 2 development, a coating which contained delta phase and an interfacial layer of 1.0 μm was found to contain 11.0 wt pct iron (Figure 8). This iron content value is close to the 12 wt pct saturation

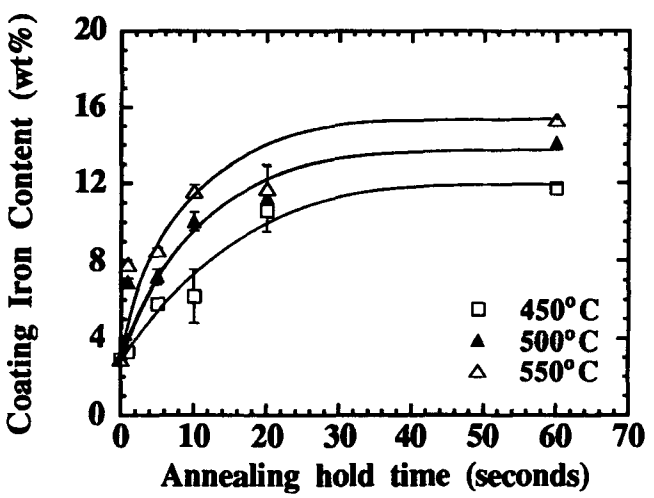

Fig. 7—Total coating iron content in weight percent as a function of annealing hold time.

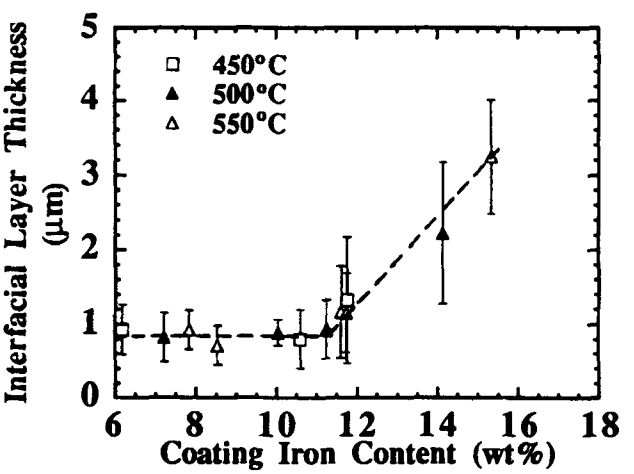

Fig. 8—Interfacial layer thickness as a function of iron content for the simulation galvannealed coatings.

limit of iron in the delta phase. Therefore, it appears that once the total coating iron content reached 11.0 to 12.0 wt pct, the delta phase would have to become supersaturated in iron in order for more iron to be found in the delta layer. According to the equilibrium Fe-Zn phase diagram (Figure 1), as the coating is annealed isothermally and the iron content of the coating continues to increase such that the iron content corresponds to a two-phase delta + gamma region, the interfacial layer is expected to nucleate and grow at the delta/gamma interface. By the rules of the phase diagram, as iron content continues to increase, the volume fraction of gamma also increases, resulting in the growth of the interfacial gamma layer. Because interfacial layer growth was observed, it is believed that in order to accommodate the influx of iron atoms during annealing, the interfacial $gamma_1/gamma_2$ layer has to grow (in preference to delta phase becoming supersaturated) and consume the delta-phase layer for the necessary zinc atoms to form the Fe-Zn $gamma_1$ and/or $gamma_2$ phase.

In this third stage of interfacial layer development, the total iron content in the coating may be estimated from the following law of mixtures expression:

$$Fe_{total} = V_\delta \cdot Fe_\delta + V_{\Gamma 1} \cdot Fe_{\Gamma 1} \quad [3]$$

where V_δ = volume fraction of delta in the coating;
$V_{\Gamma 1}$ = volume fraction of $gamma_1$ in the coating;
Fe_δ = 9.5 wt pct (average Fe solubility in delta at 300 °C); and
$Fe_{\Gamma 1}$ = 25.2 wt pct (average Fe solubility in $gamma_1$ at 300 °C).

In order to simplify the analysis, Eq. [3] assumes an interfacial layer consisting entirely of $gamma_1$ phase. This equation can be used to estimate the iron content of the fully alloyed coating based upon metallographic observation and X-ray diffraction data. For example, the 550 °C–60-second anneal sample had an interfacial layer thickness of 3.25 μm, according to Figure 6. Because a typical coating thickness was approximately 10 μm, a coating having an interfacial layer thickness of 3.25 μm (32.5 vol pct) would have a delta-layer thickness of 6.75 μm (67.5 vol pct). For this coating, the total coating iron content can be estimated as

$$(0.675)(9.5) + (0.325)(25.2) = 14.60 \text{ wt pct Fe}$$

The results of this calculation agree closely with the data shown in Figure 7, as the estimated iron content at 550 °C for a 60-second anneal (14.60 wt pct) is close to the actual measured data point of 15.2 wt pct.

The iron content data in Figure 7 (and the metallographic results in Figure 5) indicate that once the delta layer has grown to the coating surface, iron content of the coating increases only slightly due to the growth of the interfacial layer. The delta phase is present in a larger volume percent than the interfacial layer; therefore, it follows that the $gamma_1/gamma_2$ interfacial layer growth resulting from a 60-second anneal only slightly increases the total coating iron content (Figure 7). This small change in iron content after long time annealing results in a plateau region in the iron content data, as shown in Figure 7.

During this final stage of development, the interfacial layer begins to grow at an increased rate at the expense of the delta layer. Significant growth of the interfacial layer occurred once a type-1 morphology had formed (the overlay eta-phase layer had been consumed) and saturation of the delta layer had occurred. These results support the theory that the initially formed zeta + delta phase layer first grows rapidly as iron content in the coating increases. With the disappearance of the eta phase and continued diffusion, the zeta + delta phase layer transforms to an all delta layer and serves as the zinc-rich portion of a finite solid-solid Fe-Zn diffusion couple. Once the coating reached approximately 12 wt pct iron, growth of the interfacial layer became active. With the saturation of the delta layer and continued zinc and iron interdiffusion, the interface of the gamma/delta layer progresses into the delta layer. This growth was promoted by elevated isothermal annealing temperatures and an existing iron concentration gradient within the coating. Because the morphology development is independent of interfacial layer thickness, the rate of zinc and iron interdiffusion, not interfacial gamma layer growth, controls morphology development.

F. *Powdering*

In order to study the effect of interfacial layer development on coating formability properties, 60 deg bend tests were performed on the simulated coatings. The relationship between the degree of powdering and interfacial layer thickness is shown in Figure 9. Although no definitive correlation exists between the degree of powdering and interfacial layer thickness, there does appear to be two distinctly different regions in Figure 9. The first region, having an interfacial layer thickness less than or equal to 1.0 μm, indicates an insensitive relationship between interfacial layer thickness and powdering. The second region, having an interfacial layer thickness equal to or greater than 1.5 μm, shows that as the interfacial layer thickness increases, there is a corresponding increase in the amount of powdering. A change in the degree of powdering occurred at an interfacial layer thickness of approximately 1 μm. The change in powdering behavior at an interfacial layer thickness of 1.0 μm is an

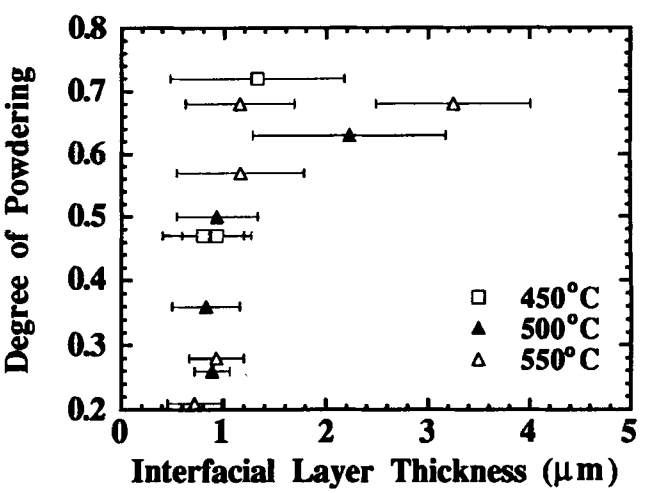

Fig. 9—Degree of powdering as a function of interfacial layer thickness for the simulation galvannealed coatings.

implicit boundary between the two regions of data presented in Figure 9.

For a 1.0-μm interfacial layer, the amount of powdering from a 60 deg bend test varied from light absorbance values of 0.25 to 0.5 (Figure 9), thus indicating that the interfacial layer thickness alone may not determine powdering properties. Both Figures 8 and 9 show a range of iron content and powdering data for coatings having an average interfacial layer thickness of 1.0 μm. These data correspond to stage 2 of interfacial layer development in which iron content in the coating increases with no accompanying growth of the interfacial layer.

The scatter in the powdering data for coatings containing a 1.0-μm interfacial layer may be due to a transition from a delta + zeta to an all delta phase layer above the interfacial layer. Figures 5 through 7 show that for coatings containing a 1.0-μm interfacial layer thickness, coating iron content increased with the densification and saturation of the delta phase. Powdering therefore is also related to whether any zeta phase remains in the coating structure, and to what degree iron saturation of the delta phase layer has occurred.

Figure 9 does indicate, however, that at an average interfacial layer thickness of 1.0-μm coating properties may change. All of the type-1 morphologies for the IF steel had interfacial layers less than 1.0 μm in thickness. Those coatings having an interfacial layer greater than 1.0 μm were type-2 structures. Therefore, an interfacial layer thickness of greater than 1.0 μm can be used as an indicator of a type-2 morphology.

The increase in powdering observed in the second region of Figure 9 for the type-2 coatings is probably due to a number of factors. As previously reported,[7] powdering and iron content were found to increase as the coating structure progressed from a type-0 to type-2 morphology. Other investigators[19,20] have also shown that the basal planes of the delta phase are preferentially oriented perpendicular to the steel substrate. This orientation of the delta phase was found to adversely affect coating structural integrity, because the type-2 coatings contained cracks along delta phase basal planes[21] prior to bend testing. Cracks in the delta phase are most likely due to phase transformation volume changes that occur within the coating during annealing. Upon 60 deg bending, this cracked type-2 coating structure contains a relatively high amount of iron (15 wt pct) and an interfacial layer greater than 1.0 μm in thickness. Cracks in the delta phase, a high coating iron content, and an interfacial layer thickness greater than 1.0 μm all contribute to the poor powdering properties of the type-2 morphology.

Although a 1.0-μm interfacial layer itself was associated with a range of powdering data (Figure 9), an implicit boundary between good and poor powdering performance is associated with this value of interfacial layer thickness. A type-1 morphology is desirable because it is a completely alloyed coating which contains a thin interfacial layer and little or no cracking along delta phase basal planes; it also has a relatively low iron content. All type-1 structures had an interfacial layer equal to or less than 1.0 μm and exhibited the least amount of powdering during bending. Interfacial layer thickness is useful as a indicator of coating formability, because coatings which contain thick interfacial layers are invariably associated with poor formability characteristics such as delta phase cracking and high iron content. Thus, the interfacial layer can be used as a morphology marker, and for optimum coating formability properties, the interfacial layer should be kept below 1.0 μm in thickness.

IV. CONCLUSIONS

A study of interfacial layer growth of galvannealed coatings on Ti-stabilized IF steel led to the following conclusions.

1. Interfacial layer development in galvannealed coatings on titanium-stabilized IF steels followed a three-stage growth process with annealing time. During the first stage of growth, there was a rapid increase in interfacial layer growth, followed by a steady-state region with almost no growth (second stage), and finally an increase in the growth rate once again during the third stage of growth.
2. Although the interfacial layer is present even at short annealing times, it does not hinder zinc and iron interdiffusion in the coating.
3. Total iron content of the galvannealed coatings first increased rapidly up to an average interfacial layer thickness of 1.0 μm, however, once the coating had reached a total iron content in excess of 11.0 wt pct, interfacial layer growth became active and coating iron content increased only slightly with continued annealing.
4. Although a strong cause and effect relationship was not found to exist between powdering and interfacial layer thickness, results of the 60 deg bend tests did show that as the interfacial layer thickness increased beyond 1.0 μm, powdering also increased. Therefore, a 1.0-μm interfacial layer thickness can be used as an indicator of powdering performance, because a thick interfacial layer is accompanied by other coating characteristics that may be deleterious to powdering resistance, such as a high iron content and cracking of the delta phase.
5. A type-1 coating morphology, with an interfacial layer thickness of less than 1.0 μm, was found to be the optimum structure for a fully alloyed coating with good powdering resistance properties.

ACKNOWLEDGMENTS

The authors would like to thank National Steel, Armco Steel, LTV Steel, Dofasco, Rouge Steel, Cockerill-Sambre, and Noranda for their sponsorship of this work. The metallographic assistance of A.O. Benscoter at Lehigh University, the Gleeble operation assistance of J. Worobec at Dofasco, and the careful editing of Professor F. van Loo, Eindhoven Technical University, and S. Attanasio, MIT, are also greatly appreciated.

REFERENCES

1. M. Urai, M. Terada, and S. Nomura: *Proc. Int. Conf. on Zinc and Zinc Alloy Coated Steel Sheet (GALVATECH)*, ISIJ, Tokyo, Japan, 1989, pp. 478-84.

2. *ASM Handbook*, ASM INTERNATIONAL, Materials Park, OH, 1992, vol. 3, p. 206.
3. J. Inagaki, S. Nakamura, M. Yoshida, and A. Nishimoto: SAE Technical Paper No. 890349, SAE Inc., Warrendale, PA, 1989.
4. S. Nakamura: *Trans. Iron Steel Inst. Jpn.*, 1986, vol. 26 (1), p. B-22.
5. T. Nakamori and A. Shibuya: *Proc. ASM World Metal Congress*, ASM INTERNATIONAL, Chicago, IL, 1988, pp. 139-49.
6. K. Onizawa, A. Yasuda, H. Koumura, K. Yamato, and H. Ota: *Proc. ASM World Metal Congress*, ASM INTERNATIONAL, Chicago, IL, 1988, pp. 45-53.
7. C.E. Jordan, K.M. Goggins, and A.R. Marder: *Proc. Second International Zinc and Zinc Alloy Coated Steel Sheet Conference (GALVATECH)*, Verlag Stahleisen, Amsterdam, The Netherlands, 1992, pp. 137-41.
8. G.F. Bastin, F.J.J. van Loo, and G.D. Reick: *Z. Metallkd.*, 1974, vol. 65, pp. 656-60.
9. G.M. Smith, D.W. Gomersall, and D.M. Hreso: *31st Mechanical Working and Steel Processing Proceedings*, Iron and Steel Society, Warrendale, PA, 1990, pp. 17-30.
10. W. Warnecke and W. Muschenborn: *Proc. 1st Int. Conf. on Zinc Coated Steel Sheet*, Zinc Development Association, Munich, Germany, 1985, pp. 16/1-16/27.
11. Y. Suemitsu, M. Nakayama, Y. Numakura, T. Kanamaru, H. Hayashi, and T. Honda: U.S. Patent No. 5049453, Sept. 1991.
12. S. Boston: Armco Research Center, Middletown, OH, private communication, 1990.
13. H. Guttman, S. Belisle, and M. Gagne: *Proc. 3rd Int. Conf. on Zinc Coated Steel Sheet (INTERGALVA)*, Association Tecnica Espanola de Galvanizacion, Barcelona, Spain, 1991, pp. S4D/1-S4D/18.
14. C.E. Jordan, K.M. Goggins, A.O. Benscoter, and A.R. Marder: *Mater. Characterization*, 1993, vol. 31, pp. 107-14.
15. S.T. Bluni, K.M. Goggins, B.S. Smith, and A.R. Marder: ASTM Special Technical Publication 1165, Philadelphia, PA, 1992, pp. 254-65.
16. K.M. Goggins and A.R. Marder: SAE Technical Paper No. 920175, SAE Inc., Warrendale, PA, 1992.
17. C.E. Jordan and A.R. Marder: *Metall. Mater. Trans. A*, 1994, vol. 25A, pp. 937-48.
18. J. Inagaki, M. Morita, and M. Sagiyama: *Surf. Eng.*, 1991, vol. 7, pp. 331-39.
19. G.F. Bastin, F.J.J. van Loo, and G.D. Reick: *Z. Metallkd.*, 1976, vol. 67, pp. 694-98.
20. V. Rangarajan, C.C. Cheng, and L.L. Franks: *Surf. Coat. Technol.*, 1993, vol. 56, pp. 209-14.
21. K.M. Goggins: Master's Thesis, Lehigh University, Bethlehem, PA, 1991.